Performance Evaluation of a Respirator Vortex Cooling Device

Ashley D. Elizondo
Savannah River Nuclear Solutions
Savannah River Site, Aiken, SC 29808
ashley.elizondo@srs.gov

Robert K. Iacovone, III
Savannah River National Laboratory
Savannah River Site, Aiken, SC 29808
robert.iacovone@srnl.doe.gov

Abstract

The United States Department of Energy's Savannah River Site (SRS) in Aiken, South Carolina is dedicated to promoting site-level, risk-based inspection practices to maintain a safe and productive work environment. Protective suits are worn by personnel working in contaminated environments. These suits require that cooling be applied to keep the interior temperature within safe and comfortable limits. A vortex tube, also known as the Ranque-Hilsch vortex tube, can provide the necessary cooling. As mechanical devices void of moving components, vortex tubes separate a compressed gas into hot and cold streams; the air emerging from the "hot" end reaching a temperature of 433.2 K, and the air emerging from the "cold" end reaching a temperature of 241.5 K. (Hilsch, 1946, "Die Expansion Von Gasen Im Zentrifugalfeld Als K€alteprozeß," Z. F€ur Naturforsch., 1, pp. 208–214). Routing the cold stream of the vortex tube to the user's protective suit facilitates the required cooling.

Vortex tubes currently in use at SRS are pre-set, through modification solely by and within the SRS Respiratory Equipment Facility (REF), to provide a temperature reduction between 22.2 and 25.0 K. When a new model of vortex tube capable of user adjustment during operation recently became available, prototype testing was conducted for product comparison. Ultimately, it was identified that similar cooling performance between the old and new models is achievable. Production units were acquired to be subjected to complete product analysis at SRS utilizing a statistical test plan. The statistical test plan, data, thermodynamic calculations, and conclusions were reviewed to determine acceptability for site use.

1   Introduction

The vortex tube, also known as the Ranque-Hilsch vortex tube (RHVT)[1], is a mechanical device operating void of mobile components which separates a compressed gas of homogeneous temperature into hot and cold fluid streams. The separation of streams in the vortex tube allows it to function as a refrigeration or heating device,

---

[1] The Ranque-Hilsch vortex tube (RHVT) was invented by French physicist Georges Ranque in 1931 and further developed by German physicist Rudolph Hilsch in 1947.

respectively, reducing or increasing the temperature of an enclosure. In prior studies, it has been demonstrated that a 100 K temperature difference between the "hot" and "cold" end of the device is attainable [1,2].

The physical separation of streams by the vortex tube is achieved through the tangential injection of a pressurized gas into a partially enclosed *swirl chamber* where the fluid stream is accelerated at a high rate of rotation. Due to the conical nozzle located at one end of the tube, only the outer shell of the compressed gas (the hot fluid stream) is allowed to escape there. The remainder of the gas (the cold fluid stream) is forced to return in an inner vortex of a reduced diameter within the outer vortex, exhausting opposite the direction of the hot fluid stream (see Fig. 1).
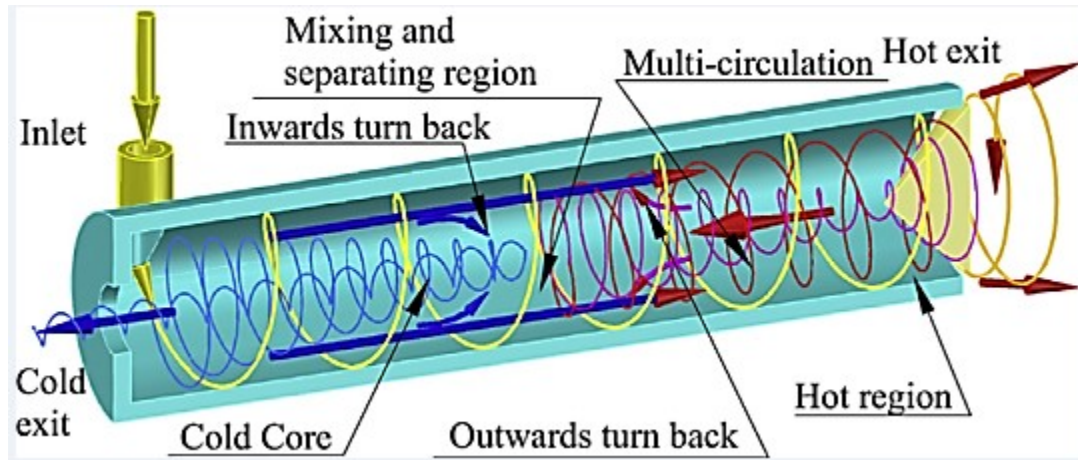

Fig. 1 Counterflow vortex tube [3]
(Fig. 1 reprinted from Int. J. Refrig. 36(6), Xue Y., Arjomandi, M., Kelso, R., The
Working Principle of a Vortex Tube, p. 1731, © 2013, with permission from Elsevier)

One theory behind the operation of a vortex tube, the "Viscous-Shear Theory," identifies that due to the natural tendency to conserve angular momentum, the concentric layers of the core of the vortex incur faster angular velocities in comparison with the outer annulus during initial travel toward the conical nozzle. The shearing effect of the fluid molecules results in the transfer of kinetic energy from the core to the outer annulus of the vortex, subsequently increasing the temperature of the vortex annulus while reducing the temperature of the vortex core [2]. This is somewhat analogous to a Peltier effect device, which uses electrical pressure (voltage) to move heat to one side of a dissimilar metal junction, causing the other side to become cold.

The primary purpose of this study is to evaluate the vortex tube in its performance as a refrigeration device, reducing the temperature within a SRS designed plastic suit airline respirator (PSAR). Remaining content within this paper includes sections on the background and purpose of using a vortex tube as a cooling device, the experimental setup, thermodynamic analysis, statistical analysis, test integrity verification, and an analysis of experimental uncertainty. The paper then concludes with a summary of findings.

2   Background

PSARs are utilized at SRS to provide protection against airborne contamination. Connecting the cold exhaust flow of a vortex tube to a PSAR allows a user to significantly reduce his/her ambient temperature in the field. Though vortex tubes are currently available for use at SRS, a new vortex tube model, model "B" (Fig. 2), became available which offers numerous potential advantages over the current model, designated as model "A." Model designations were chosen solely to protect proprietary information. One such new advantage includes the

incorporation of a preset temperature drop of 11.1 K with a user adjustable control valve and a muffler, capable of reducing the cold air stream temperature further by approximately 11.1 K, for a total temperature reduction around 22.2 K.

Fig. 2   RHVT with user adjustable control valve

Additional advantages of the new vortex tube model over the current model includes eliminating the need for initial adjustment at the SRS respiratory equipment facility (REF), providing additional suitability with the availability of 9.525-mm x 15.24-m, 30.48-m, and 45.72-m breathing air hoses, eliminating the use of heat shields or leather sleeves due to tube encasement, and increasing convenience through the addition of a belt loop on the vortex tube with an adjustable waist belt and a plastic buckle.

Testing of a model B prototype was completed by Savannah River National Laboratory (SRNL) in 2014, indicating high potential for use of this device and warranting further study. Initial prototype testing identified an achievable temperature reduction of 22.2 K; matching the cooling capability of model A vortex tubes currently in use. Therefore, 50 model B vortex tubes were ordered relative to the prototype design to be subjected to complete product testing prior to field implementation at SRS.

3   Experimental Setup

For observations of the PSAR helmet plenum volumetric airflow, an inline rotameter was mounted to a modified scaffold structure (Fig. 3) and connected downstream to a plastic suit silencer distributor (PSSD) servicing the helmet plenum and two leg air hoses. The PSSD received the cold airflow exhausted directly from the vortex tube and routed it to different locations within the plastic suit, as indicated in Fig. 4.

Twenty-five of the 50 model B production units received by SRS were randomly selected for product testing. Each of the 25 vortex tubes were labeled, numbered 1 through 25, prior to testing. Testing began by attaching a single vortex tube upstream from the PSSD and manipulating the ball valve lever to release airflow from the air manifold. An airflow regulator was then adjusted, or verified, to produce a pressure of 689.5 kPa. A structured testing procedure was developed during testing and included adjusting the RHVT control valve, muffler, to the fully closed position, ensuring that the rotameter float remained unaffected by excessive friction between the float and the guide rod, thus allowing adequate time for the system to recover from the effects of hysteresis prior to collecting data. Incorporating this structured testing procedure, the helmet plenum

volumetric airflow data point collected for when the muffler was in the closed position occurred after the RHVT was closed completely, then opened slowly and exactly to the point where the vortex tube ceased producing undesirable whistling noise. The muffler was then opened completely and the volumetric airflow data point was again recorded. Following the collection of the helmet plenum volumetric airflow data points, the control valve was returned to the closed position. The PSSD was disconnected from the RHVT and an alternate rotameter was attached directly to the RHVT. For the same previously described open and closed positions of the control valve, the total cold stream volumetric airflow data points were similarly recorded.

Following the collection of all volumetric airflow data points, a Cejn[2] test apparatus was attached to the vortex tube. This test apparatus consisted of a 9.525-mm diameter Cejn 342 Series quick release fitting with a 5.08-cm long segment of 9.525-mm diameter breathing air hose attached to the ribbed end of the fitting, as seen in Fig. 5. With the inlet air stream adjusted to 689.5 kPa, the temperature of the cold stream was then measured at a specified point on the 5.08-cm segment of breathing air hose (delineated by a black marking on the outer surface of the Cejn test apparatus), utilizing a Fluke[3] thermometer, as shown in Fig. 6. Then, after adjusting the muffler to the fully open position, a stopwatch began tracking the test trial time, and the initial cold airflow temperature was recorded. After 10 and 20 minutes of continuous airflow through the vortex tube, the second and final cold stream temperatures were recorded. The procedure was then repeated in entirety with the remaining 24 RHVTs. (Note that, for all cases in which the cold air stream temperatures were collected, the ambient temperature was recorded prior to commencing testing.)

---

[2] The Cejn Industrial Corporation of Gurnee, Illinois, is a manufacturer of air supply hoses and quick release fittings.

[3] Fluke Calibration of Everett, Washington, is a manufacturer of calibration test equipment.

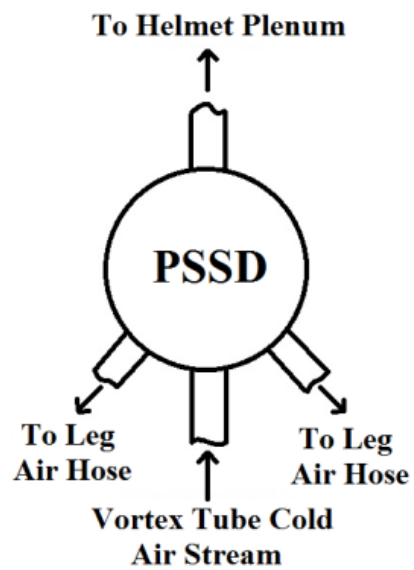**Fig. 3   Vortex tube testing station**

Fig. 4 The PSSD receives the cold air stream from the vortex tube and distributes fractions of the cold stream to the helmet plenum and leg air hoses

Fig. 5 The Cejn test apparatus consisted of a 9.525-mm diameter Cejn quick disconnect fitting attached to a small length of breathing air hose

Fig. 6 A Fluke 51 II thermometer was utilized to collect air temperature measurements during testing

Five of the 25 previously tested RHVTs were then randomly selected and again subjected to the same initial testing procedure at 689.5 kPa. The 5 RHVTs were evaluated for the rate of volumetric airflow and air temperature of the exhausted cold stream. After collection of all data with the inlet air pressure corresponding to 689.5 kPa, the pressure was increased to 827.4 kPa. The initial testing procedure was then replicated for each of the five randomly selected vortex tubes and data recorded.

Subsequent to the completion of all time trials analyzing the vortex tube cold air stream temperatures, all 25 vortex tubes were placed individually into a SRNL designed Plexiglas®[4] airflow chamber, as shown within Fig. 7. The entire perimeter of the cover was sealed using weather stripping material, pressure-sensitive adhesive-backed foam, allowing air to only flow out of the box at a single orifice. An in-line mass flow transmitter, connected to the box orifice, then measured the total volumetric airflow (the combined hot stream and cold stream) exhausted from the vortex tube. (For each of the collected total volumetric airflow measurements, the inlet airflow corresponded to a test pressure of 689.5 kPa.)

Fig. 7 A Plexiglas® airflow chamber was used to measure the total volumetric rate of airflow through a RHVT

A final collection of data evaluated the noise level present within the PSAR helmet during the use of a vortex tube. This testing utilized five plastic suits (excluding the pants for all cases) and 15 (of the 25 previously tested RHVTs) randomly selected vortex tubes (chosen in accordance with ANSI/ASQ Z1.4 lot quality assurance sampling for a lot size of 50 units) [4]. (See Fig. 8 for the experimental setup utilized during sound testing.) Testing included the analysis of each vortex tube for three different suit sizes; two extra-large, two tween, and one large. Data samples were collected with a sound level meter during this test procedure respective to inlet air pressures of both 689.5 kPa and 827.4 kPa.

---

[4] Plexiglas® is a registered tradename of Arkema of Colombes, France.

Fig. 8 Experimental setup for PSAR jacket and helmet noise level test

4   Thermodynamics Analysis

The model B production unit performance as a refrigeration device was evaluated for its ability to reduce the internal temperature of a site designed PSAR. The performance of the vortex tube as a refrigeration device was evaluated using the relationship defined within Eq. (1), treating the enclosure as an open system control volume,

$$\beta = \frac{\dot{Q}}{\dot{W}} \tag{1}$$

for which β is the coefficient of performance (COP), $\dot{Q}$ is the refrigeration effect of the vortex tube, and $\dot{W}$ is the work done to compress the air from atmospheric pressure and temperature to the vortex tube inlet conditions, located downstream the air manifold pressure regulator at the breathing air hose quick release fitting (see Fig. 3). The refrigeration effect of the vortex tube is defined by the relationships in Eq. (2)

$$\dot{Q} = \Delta\dot{H}_c = \dot{m}_c C_p (T_i - T_c) \tag{2}$$

Here, the refrigeration effect of the vortex tube is identified to be the change in enthalpy, $\Delta\dot{H}_c$, in the exhausted cold stream; calculated as the product of the mass flow rate of the cold stream, the specific heat of air at constant pressure, and the difference in the inlet stream and cold stream temperatures, respectively $\dot{m}_c$, C_p, T_i, and T_c.

8

The work done by the compressor is defined in Eq. (3)

$$\dot{W} = \dot{m} C_p T_2 \ln\left(\frac{T_2}{T_1}\right) \tag{3}$$

where T_1 and T_2 are the respective compressor inlet and exit temperatures $\dot{m}$ is the mass flow rate, and a reversible isentropic process is assumed. An isentropic model is chosen to represent the compressor side of the vortex tube to bound the amount of compression work measured by the temperature change of the compressed fluid. For small temperature differences, the equation of the work done by the compressor (in terms of power) simplifies to the relationship in Eq. (4)

$$\dot{W} = \dot{m}_i C_p (T_2 - T_i) \tag{4}$$

Here, the product of the rate of change of the mass flowing into the system, $\dot{m}_i$, the specific heat of air at constant pressure, and the difference of the temperature of air following compression, T_2, and the temperature at atmospheric conditions, T_i, are used to calculate the ideal work needed to drive the compressor.

The time rate of flow of mass of the RHVT cold exhaust stream was calculated, in each case, as the product of the measured volumetric flow rate of the cold air stream and the density of the air at the corresponding temperature value and relative air humidity, as in Eq. (5)

$$\dot{m}_c = \dot{V}_c * \rho(T_c) \tag{5}$$

where $\dot{V}_c$ refers to the volumetric flow rate of the cold air stream and $\rho(T_c)$ is the density of air at the corresponding cold air temperature.

Calculated coefficients of performance identified results similar to actual COP values contained within published literature [5]. Numerical data indicated that the devices are highly irreversible, with corresponding COP values around 0.075. Despite these low COP values, when a steady supply of compressed air is readily available, a vortex tube is a viable solution for spot cooling or reducing the temperature of a small enclosure. (It should be noted that the COP values from Ref. [5] are based on an isothermal rather than an isentropic compression model. The difference between these two measures has a very limited effect on the calculated COP).

Average values of the refrigeration effect and work done by the compressor (in terms of power) were found equivalent to 0.19 kW and 2.58 kW, respectively. The calculated average value of the refrigeration effect, 0.19 kW, was used in comparison of the production unit performance to the supplier's published product specifications of similar models. The tested production units were found to exceed the supplier's minimum expected refrigeration effect, approximately 0.13 kW.

5   Statistical Analysis

The attainable temperature drop of model B RHVTs was evaluated through product testing as a function of cooling time. Product testing determined that the average temperature reduction from ambient conditions was approximately 16.8 K; 11.1 K preset by device design (where the muffler control valve is in the fully closed position) and an additional reduction of approximately 5.7 K adjustable by the user (when the muffler control valve is in the fully open position). Also demonstrated was that only PSARs which utilize helmets containing enhanced noise suppression material (currently found in tween and extra-large sizes) are capable of maintaining a noise level below 80 dBA while using the new model of vortex tube. Maintaining a noise level below 80 dBA

mitigates the risk of noise induced hearing loss; as identified by OSHA 29 CFR Part 1926 [6] and NIOSH criteria [7].

Internal SRS Respirator Protection Manual specifications require that a volumetric airflow ranging between 25.43 Sm^3/h to 42.38 Sm^3/h be supplied to the PSAR to maintain an assigned protection factor (APF) of 10,000 [8] as approved through the United States of America, Department of Energy (DOE). Testing identified that the sample set's total cold volumetric airflow measurements averaged 32.61 Sm^3/h. Additionally, all collected cold volumetric airflow measurements ranged between 30.51 Sm^3/h and 33.9 Sm^3/h; meeting SRS respirator program manual specifications for PSARs. In addition to the minimum airflow required to service the suit, the PSAR helmets require that airflow between 10.17 Sm^3/h and 16.95 Sm^3/h be supplied to the helmet plenum to provide an APF of 10,000 as approved through the DOE. With the collected volumetric airflow measurements for the helmets ranging between 17.63 and 19.32 Sm^3/h, the internal SRS specification for helmet plenum airflow was exceeded. Nevertheless, the minor increase in the volumetric airflow supplied to the helmet plenum still maintains an APF of 10,000. Therefore, despite exceeding the SRS respiratory program manual specifications for PSAR helmet plenum airflow, the tested product is still considered acceptable for use.

Data analysis was conducted with JMP Statistical Software [9]. At the conclusion of 20 minutes of testing with uninterrupted airflow through each vortex tube at 689.5 kPa, the temperature drop (Diff20) between ambient room conditions was determined. The temperature drop from RHVT #16 (lowest point in Fig. 9) was determined to be an outlier due to manufacturer quality and assembly issues that have been remediated. Therefore, it was not included in further statistical analysis.

The data contained in Table 1 summarized the statistical results for the temperature drop relative to ambient room temperature initially (Diff00), after 10 (Diff10), and 20 minutes (Diff20). The statistics include the mean, standard deviation, and 95% error limits for the mean. The average cold air stream temperature drop of the vortex tube was 16.8 K (Table 1). Individual measurements ranged between 15.3 and 18.4 K.

Considering that the largest drop in temperature from ambient conditions occurred for the data set collected after 20 minutes of continuous airflow, it remains the data of current focus. At 20 test minutes, a mean of 16.8 K and a standard deviation of 0.89 K produced a 95% confidence interval of 16.4 K to 17.2 K for the n=24 test units; meaning that a repeat test of the entire sample set would result in newly calculated mean values between these lower and upper bounds with 95% confidence.   The difference in temperature drop from the initial measurement to 10 minutes (Del 00 10) was 0.54 K on average and is significant (Table 2) as determined by the 95% confidence interval (0.32, 0.76). However, the difference in the average temperature drop between 10 and 20 minutes (Del 10 20) was not significant.

A statistical process control (SPC) chart for Diff20 (Fig. 10) plotted according to the test sequence shows no trends or patterns over the experimental campaign indicating that the data were essentially random.
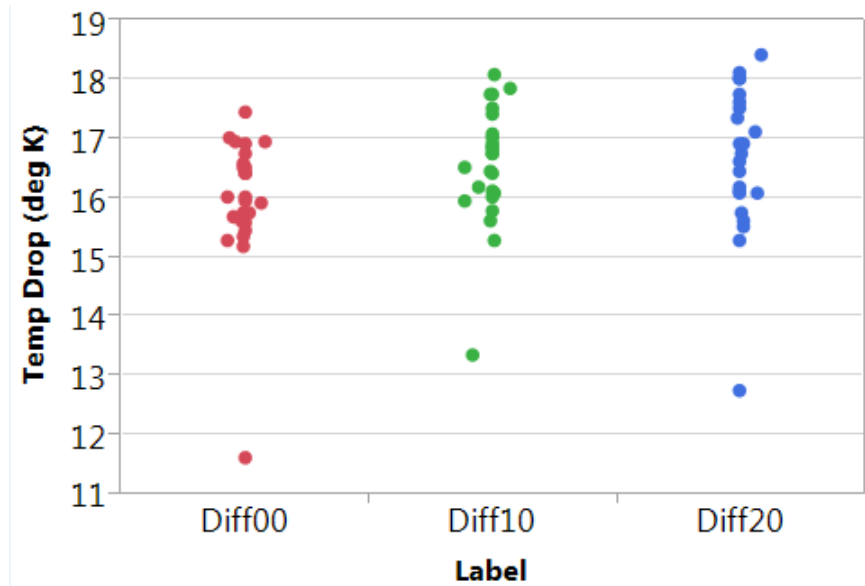
Fig. 9 Temperature drop relative to ambient room temperature (K) initially, after 10 and after 20 minutes
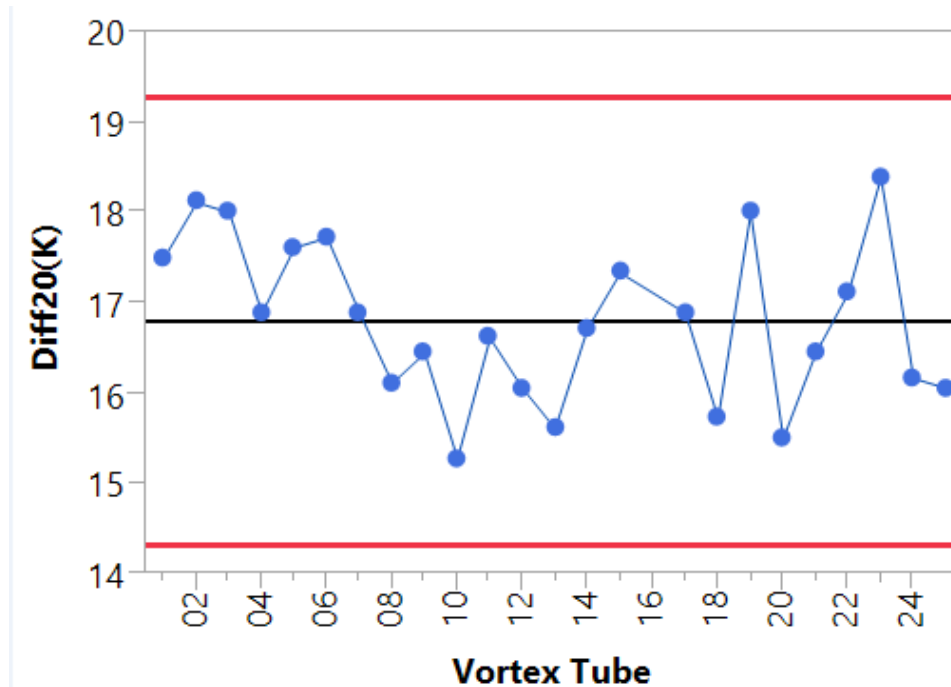

Fig. 10 SPC Chart of temperature drop relative to ambient room temperature (K) at 20 min (Diff20)

Table 1: The statistical values for the 24 RHVT Sample set collected for analysis

Label	N	Mean	Std Dev	Lower 95% Mean	Upper 95% Mean
		(K)	(K)	(K)	(K)
Diff00	24	16.15	0.64	15.88	16.42
Diff10	24	16.69	0.75	16.37	17.01
Diff20	24	16.8	0.89	16.42	17.18

Table 2: Sample Statistics for RHVT test data

Statistic	Del 00 10 (K)	Del 10 20 (K)	Del 00 20 (K)
Mean	0.54	0.11	0.65
Std Dev	0.52	0.41	0.60
Std Err Mean	0.11	0.08	0.12
Lower 95% Mean	0.32	-0.06	0.39
Upper 95% Mean	0.76	0.28	0.90

A Normal Quantile Plot (NQP) (Fig. 11) was used to visualize the extent to which Diff20 is normally distributed. The NQP, also called a quantile-quantile plot, or Q-Q plot, shows 95% confidence bounds [10] and both the probability and normal quantile scales. This NQP also indicates that Diff20 can be modeled by a normal distribution, because the points of the NQP can be approximated by a straight line. The p-values for good-of-fit statistics for the normal distribution are 0.76, 0.61, and 0.30 for the Anderson-Darling, Shapiro-Wilk, and the Skewness-Kurtosis test, respectively. Additionally, other probability distributions were identified using Distribution Analyzer [11] through use of a Skewness-Kurtosis Plot (Fig. 12) and found to give reasonable representations of the data.
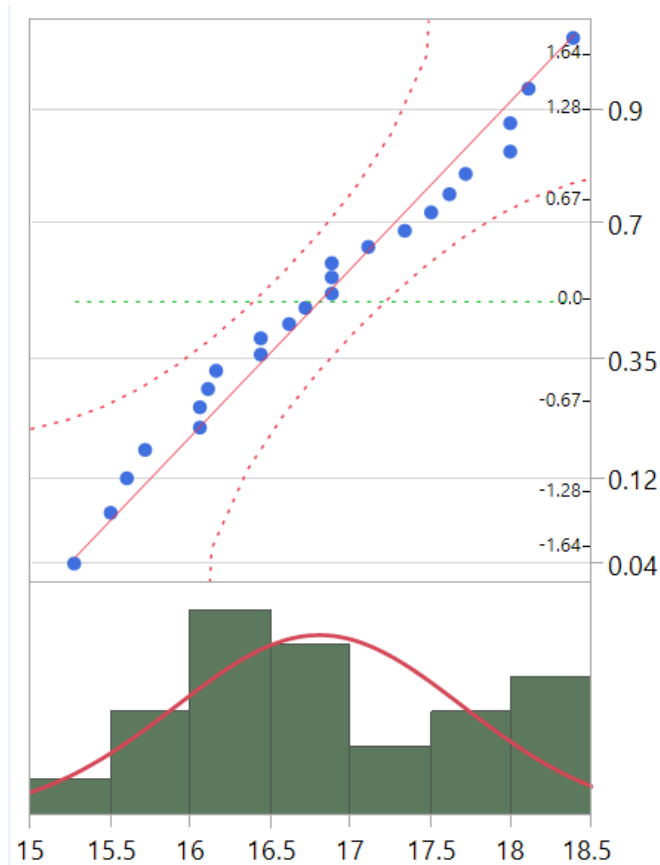
Fig. 11 Normal quantile plot, histogram, and fitted normal distribution for Diff20 (K)
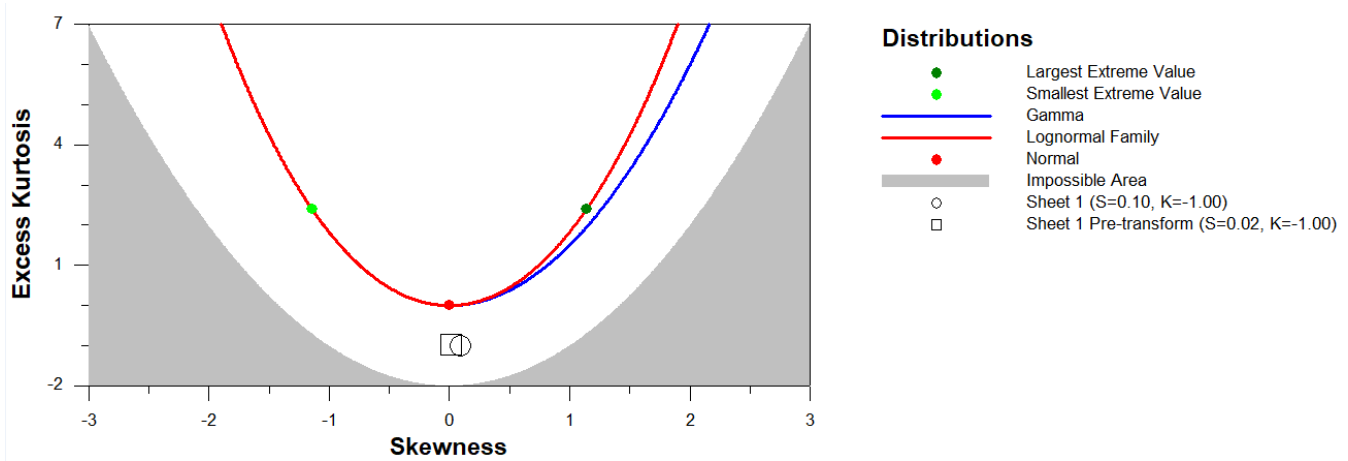
Fig. 12 Skewness-Kurtosis plot for Diff20 data

The normal distribution, largest and smallest extreme value distribution are represented by a single point on a Skewness-Kurtosis Plot (Fig. 12); whereas the lognormal and gamma distribution are represented by curves. The impossible region where no distribution can fall is shaded gray. Distributions closest to the data (Sheet 1) in the Skewness-Kurtosis Plot are selected as possible distributions representing the data.

The skewness (the third central moment) is a measure of the symmetry of the distribution. Because the normal distribution is a symmetric distribution, the skewness is zero. The Largest Extreme Value distribution is skewed to the right and, therefore, has a positive skewness. The Smallest Extreme value distribution is skewed to the left and has a negative skewness. Kurtosis (the fourth central moment) is a measure of whether the data are heavy-tailed or light-tailed relative to a normal distribution. As such, the normal distribution has an excess kurtosis (kurtosis-3) of zero. For excess kurtosis, defined as kurtosis–3, greater than zero indicates that the distribution tails are heavier than the normal distribution, while a value less than zero indicates that the tails are lighter than the normal distribution.

The goodness of fit tests [12] reject the hypothesis of normality when the p-value is less than or equal to 0.05. Failing the normality test allows one to state with 95% confidence that the data does not fit the normal distribution. Passing the normality test only indicates that no significant departure from normality was found. Similar statements apply to any other assumed probability distribution. With the idea of robustness, a number of probability distributions can be used to represent the data (Table 3). None of the probability distributions in Table 3 can be rejected according to their p-values (in comparison with the threshold value p=0.05). Over the five probability distributions, the lower tolerance limit for 99% coverage (with 95% confidence) is 13.7 K, and the upper limit is 20.6 K.

Table 3: Tolerance Intervals for temperature drop with 99% Coverage and 95% Confidence

Distribution	Lower TI	Upper TI	p
Normal	13.68	19.91	0.30
Largest Extreme Value	13.99	19.33	0.38
Smallest Extreme Value	14.65	19.91	0.44
Gamma	14.30	20.63	0.37
lognormal	14.08	20.38	0.33

13

6   Test Integrity Verification

The experiments were conducted over the course of two days. Lower ambient room temperatures were observed in the morning hours of testing and both higher and plateauing temperatures were observed in the afternoon (Fig. 13). The overall ambient temperature range was between 293.4 and 296.3 K. A plot of the temperature reduction (Diff20) versus ambient room temperature (Fig. 14) demonstrated independence between the two variables.
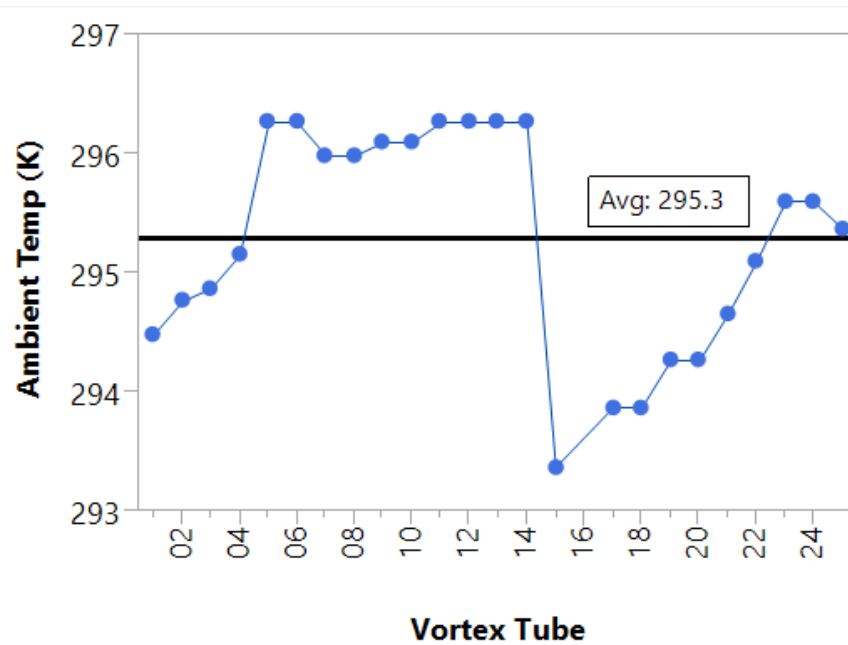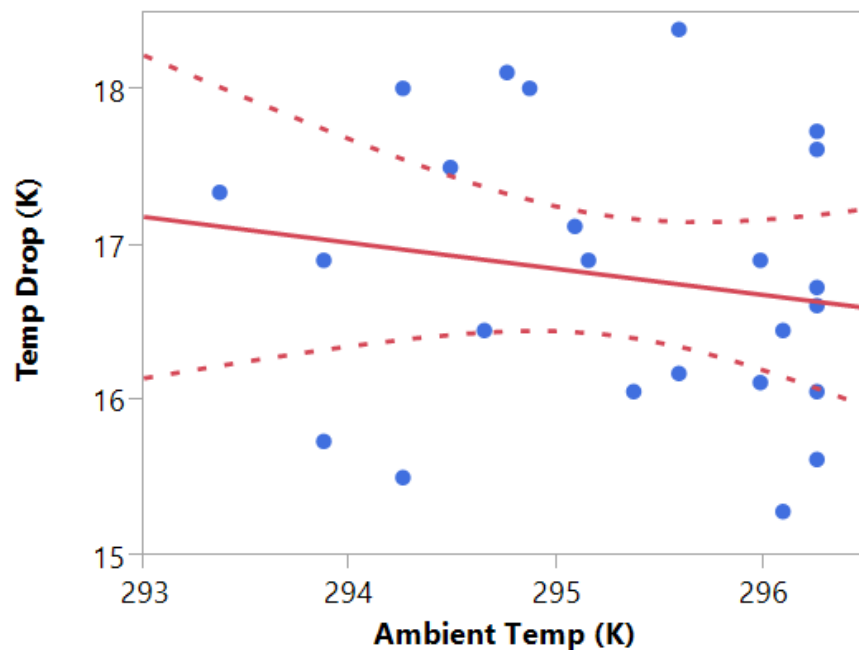

Fig. 13 Ambient room temp (K) vs RHVT

Fig. 14 Diff20 vs. ambient temp (K)

14

In theory, the temperature reduction should not be grossly affected by the ambient room temperature. The temperature reduction should be calculated utilizing the temperature of the inlet air stream for which the compressed air would normalize to, and correspond with, the atmospheric temperature prior to use within the testing facility, because the air reservoir was located outside the testing facility. However, the SRS-approved experimental test setup did not allow for obtaining temperature measurements of the air prior to entering the RHVT. Therefore, results were calculated assuming that the ambient room temperature varied in accordance with the atmospheric temperature throughout the day. To perform the calculations, local atmospheric conditions corresponding to the time experimental proceedings took place were obtained from the SRNL Meteorological Center.

The calculated results in temperature reduction displayed no correlation to ambient temperature primarily due to unavoidable inconsistencies within the testing procedure. The vortex tube manufacturer's design omitted the incorporation of a definite location for which the control valve was in the fully open position. Minor variance in the machining of the control valve screw threads would allow for alternate fully open control valve settings to be utilized during testing affecting the fraction of hot airflow. For each test, the open position of the control valve was dependent upon the test administrator's feel for where the screw threads reached maximum resistance; this may have been affected by the quality or cleanliness of the machined screw threads of each RHVT.

The manufacturer's product design and assembly process, examined for remediation, further limited the fraction of hot airflow. Reduced volumetric airflow rates of the hot air stream, potentially caused by overly compact steel mesh within the muffler or by fabricating the control valve to an incorrect, smaller, orifice size, were presumed to explain the noticeable difference in the maximum achievable reduction of temperature in the cold air stream of the vortex tube.

Disassembly of the muffler by the manufacturer identified the dimension of the control valve orifice diameter of concern, designated "orifice A." The prototype units were to be fabricated with control valve orifice diameters, designated "orifice B," 32 percent larger than the measured dimension of "orifice A." Therefore, two RHVTs were returned to the manufacturer for replacement mufflers with units containing control valve orifices matching the prototype dimensions. Upon return to SRS, the two repaired RHVTs were evaluated for their performance in accordance with the initial test plan. The reduced performance assumption was validated during retesting when the two units were found capable of producing a cold air stream temperature approximately 22.2 K below ambient. Therefore, replacing the mufflers on all 50 production units with control valves fabricated to the dimension matching "orifice B" was necessitated. After replacing the mufflers, all production units would be retested in accordance to the initial test plan.

A test was conducted to determine the impact of airflow pressure at 689.5 kPa versus 827.4 kPa. Five vortex tubes were randomly selected from the sample set and temperature data were collected for analysis. Again, the temperature reduction after 20 minutes was determined. The Diff20 at 689.5 kPa and Diff20 at 827.4 kPa were treated as matched pair differences. The Matched Pairs platform compares the means between the two correlated variables and assesses the differences. The *paired t-test* was conducted with the results presented in Table 4. The average temperature reduction after 20 minutes at 827.4 kPa is 16.8 K and at 689.5 kPa is 17.1 K. There is no statistical difference in temperature reduction between the two pressures as indicated by the tail probability of 0.56 being not less than 0.05 for testing at the 5% level. To summarize, an increase in airflow pressure held no discernable correlation to the temperature of the cold air stream.

Table 4: Statistics for impact of pressure differences

Drop120 (K)	16.8	N	5
Drop100 (K)	17.1	Correlation	0.168
Mean Diff (K)	-0.33	t-Ratio	-0.629
Std Error (K)	0.53	DF	4
Upper 95% (K)	1.14	Prob >|t|	0.56
Lower 95% (K)	-1.81		

7 Uncertainty Analysis

The refrigeration effect of the model "B" RHVT was selected for demonstrating the propagation of uncertainty to a result. This overall analysis identifies the systematic errors present during testing and random errors identified during statistical analysis of the collected data and demonstrates how each error type contributes to the overall uncertainty. Within this calculation, the total uncertainties present in the measurements of the temperature and volumetric flow rate of the cold airflow stream, RHVT attributes of the customer's primary focus, are specifically acknowledged.

The best estimate of the true value of the RHVT refrigeration effect, $\dot{Q}'$, is given as

$$\dot{Q}' = \overline{\dot{Q}} \pm u_{\dot{Q}} \tag{6}$$

where the mean value of the result, $\overline{\dot{Q}}$, is calculated with the mean values of the component variables and where the total standard uncertainty in the result, $u_{\dot{Q}}$, is calculated with the combined measurement systematic and random uncertainties corresponding to each component variable. During this experimentation, the measured values of temperature and volumetric airflow were assumed to be subject to instrument errors and temporal variation errors only. Instrument errors were assigned a systematic uncertainty based on manufacturers' statements whereas temporal variation errors were assigned a random uncertainty based on the variation in the measured data obtained during presumably fixed operating conditions [13].

Three instruments were utilized to collect temperature and volumetric airflow rate data. For each instrument, a manufacturer's statement identifying the corresponding accuracy, or uncertainty, was available; and since not otherwise specified, each was assumed to correspond to a 95% probability level [13]. These instrument uncertainties identified by the manufacturer, B, represent systematic uncertainties ($\pm b$) present during testing. At any confidence level, the systematic uncertainty is given by $t_{v,P}b$; where $t_{v,P}$ is the t value corresponding to v degrees of freedom at the confidence level, P. The interval defined by the systematic uncertainty at the 95% probability level is defined as

$$\pm B = \pm 2b \quad (95\%) \tag{7}$$

where 2 represents the t-value, 1.96, rounded for convenience [13]. Calculation of the total expected uncertainty requires evaluation with generic systematic standard uncertainties, b. Random uncertainties, $s_{\overline{x}_i}$, are the sample standard deviation of the means; defined as

$$s_{\overline{x}_i} = \frac{s_{x_i}}{\sqrt{N}} \tag{8}$$

for each component variable sample standard deviation, s_{x_i}, and N number of samples.

Due to propagation of the systematic and random standard uncertainties through the variables, the systematic standard uncertainty of the result, b_R, and the random standard uncertainty of the result, s_R, are estimated using the root of the sum of the squares, RSS, method as shown in the following equations:

$$b_R = \left(\sum\nolimits_{i=1}^{L} [b_{\bar{x}_i}]^2 \right)^{1/2} \tag{9}$$

$$s_R = \left(\sum\nolimits_{i=1}^{L} [s_{\bar{x}_i}]^2 \right)^{1/2} \tag{10}$$

where $b_{\bar{x}_i}$ and $s_{\bar{x}_i}$ are the respective systematic and random standard uncertainties of the ith component, for L elements of error evaluated at the one standard deviation confidence level.

The total standard uncertainty of the refrigeration effect, $u_{\dot{Q}}$, evaluated at specific confidence levels through the use of appropriate t values (determined in accordance with the probability level of interest, P, and the corresponding degrees-of-freedom, v) is equivalent to the combination of the systematic and random standard uncertainties, and calculated utilizing the following equation:

$$u_{\dot{Q}} = t_{v,P} \left(b_R{}^2 + s_R{}^2 \right)^{1/2} \qquad (P\%) \tag{11}$$

Here, the degrees-of-freedom is estimated using the Welch-Satterthwaite formula [13].

Table 5 captures systematic, random, and total uncertainties calculated utilizing equations (2), (5), and (7) - (11). The reported systematic and random uncertainties correspond to a 68% confidence level. The total uncertainties are reported at a 95% confidence level. For the required calculations, values of C_p were extrapolated utilizing a table of ideal gas specific heats, located within published literature [14]. Furthermore, values for the density of air at respective cold air temperatures were estimated as calculations utilizing elevation, air temperature, altimeter, and relative humidity data provided by Savannah River National Laboratory Meteorological Center.

Table 5: Systematic, random, and total uncertainties

Systematic Uncertainty (68%)			Random Uncertainty (68%)			Total Uncertainty (95%)		
$b_{\bar{T}_i}$	0.50	K	$s_{\bar{T}_i}$	0.19	K	$u_{\dot{Q}_c}$	27.80	W
$b_{\bar{T}_c}$	0.16	K	$s_{\bar{T}_c}$	0.28	K	u_{T_c}	0.66	K
$b_{\bar{V}_c}$	1.95	$\frac{Sm^3}{h}$	$s_{\bar{V}_c}$	0.14	$\frac{Sm^3}{h}$	$u_{\dot{V}_c}$	3.94	$\frac{Sm^3}{h}$

Systematic standard uncertainties were found to have greater effect on the inlet temperature and volumetric airflow rate of the cold air stream total uncertainties, whereas the random standard uncertainty of the cold air stream temperature affected the total cold air stream temperature uncertainty more. For the combined, total uncertainty of the refrigeration effect, the uncertainty in the temperature of the cold air stream, and the uncertainty in the volumetric airflow rate of the cold air stream, t-values obtained from a table contained within

published literature [15] were utilized for calculation, corresponding to a 95% confidence level and a large value (approximately 50) for the degrees-of-freedom.

With the calculated total uncertainties, the best estimates of the model B RHVT refrigeration effect, the volumetric airflow rate of the cold air stream, and the temperature of the cold air stream were determined with 95% confidence. The best estimate of the refrigeration effect is 192.53 ± 27.80 W. The best estimate of the volumetric airflow rate of the cold air stream is 32.93 ± 3.94 Sm^3/h. Finally, the best estimate of the temperature of the cold air stream is 278.58 ± 0.66 K.

8   Conclusions

All tested model "B" RHVT production units were determined to be acceptable for use with regard to airflow. The cold stream volumetric airflow rates met or exceeded SRS Respirator Protection Manual specifications: 25.43 Sm^3/h to 42.38 Sm^3/h supplied to the PSAR PSSD, and 10.17 Sm^3/h to 16.95 Sm^3/h supplied to the PSAR helmet plenum. The average cold stream volumetric airflow supplied to the PSSD was determined to be 32.9 ± 3.94 Sm^3/h with 95% confidence.

Test data collected during the administration of alternate inlet air pressures, 689.5 kPa and 827.4 kPa, identified no discernable correlation between air pressure and the temperature of the cold air stream-explained in part by the choked flow conditions present at the inlet and outlet of the vortex tube. The choked flow fixed the velocities and flow patterns within the vortex tube, subsequently limiting the hot and cold flow ratio to a narrowed range. Nevertheless, during field use, utilizing the lower air pressure would produce a similar reduction of temperature in the cold air stream, while limiting the amount of work needed to compress the inlet air throughout operation. Limiting the inefficiency of the device by this means would subsequently provide a small cost savings.

Noise testing identified that the production units are capable of operating at a noise level below 80 dBA within a PSAR. However, the use of enhanced noise suppression material within the PSAR helmet, as currently found in the tween and extra-large size suits, is required.

Analysis of the test data indicated that the production unit's cold air stream average temperature drop from ambient room temperature after 20 minutes of continuous airflow through the vortex tube was 16.8 K. The average cold air stream temperature after 20 minutes of continuous testing was calculated to be 278.6 ± 0.66 K with 95% confidence. The average temperature drop of the production units represented 75% of the expected cooling performance with regard to the prototype performance. The reduced cooling performance of the tested production units was determined to be solely attributable to fabricating the production unit control valves to an incorrect, smaller, orifice diameter. After replacing the control valves and repeating the initial testing procedure for volumetric airflow and cold stream temperature measurements, model B production units were found capable of achieving the same cooling performance as model A units (22.2 K temperature reduction) while meeting the SRS respiratory protection manual specifications for the volumetric airflow supplied to PSARs. Therefore, supplemental testing will commence.

A more complete and diverse set of data is currently being sought at SRS to determine whether enhanced cooling can be obtained through device design changes and manufacturing improvements. Supplemental experimentation with extended testing times, incorporation of alternate breathing air hose lengths, and evaluation at elevated inlet air temperatures will provide a more complete analysis of model B RHVT product performance.

Acknowledgements

Funding Data

Nomenclature

ANSI	American National Standards Institute
APF	Assigned Protection Factor
ASME	American Society of Mechanical Engineers
ASQ	American Society for Quality
BAH	Breathing Air Hose
C	Celsius
CFR	Code of Federal Regulation
COP	Coefficient of Performance
dBA	Decibel, A-weighted measurement
Del 00 10	Temperature drop (K) from the initial temperature to 10 minutes
Del 10 20	Temperature drop (K) from 10 to 20 minutes
Del 00 20	Temperature drop (K) from the initial temperature to 20 minutes
DIFF00	Initial temperature drop (K) relative to ambient room temperature
DIFF10	Temperature drop (K) after 10 minutes relative to ambient room temperature
DIFF20	Temperature drop (K) after 20 minutes relative to ambient room temperature
DOE	United States of America, Department of Energy
F	Fahrenheit
K	kelvin
kPa	kilopascal
kW	kilowatt
NIOSH	National Institute for Occupational Safety and Health
NQP	Normal Quantile Plot
OSHA	Occupational Safety and Health Administration
PSAR	Plastic Suit Airline Respirator
psig	Pounds per Square Inch Gage
PSSD	Plastic Suit Silencer Distributor
REF	Respiratory Equipment Facility
RHVT	Ranque-Hilsch Vortex Tube
SCFM	Standard Cubic Feet per Minute
Sm^3/h	Standard Cubic Meter per Hour (defined at 288.15 K)
SPC	Statistical Process Control
SRNL	Savannah River National Laboratory

SRS   Savannah River Site
Tween   Plastic Suit Airline Respirator sizing designation between large and extra-large

References

[1] Hilsch, R., 1946, "Die Expansion Von Gasen Im Zentrifugalfeld Als Kälteprozeß," Z. Für Naturforschung, 1, pp. 208-214.

[2] Baker, P.S., and Rathkamp, W.R., 1956, "Investigations on the Ranque-Hilsch (Vortex) Tube," Oak Ridge National Laboratory Report, U.S. Atomic Energy Commission, Oak Ridge, TN, Report No. ORNL-1659.

[3] Xue, Y., Arjomandi, M., and Kelso, R., 2013, "The working principle of a vortex tube," Int. J. Refrigeration, 36(6), p. 1731.

[4] ANSI/ASQ Z1.4-2003 (R 2013), 2013, "Sampling Procedures and Tables for Inspection by Attributes," American National Standards Institute/American Society for Quality, "Tables X-H – Tables for sample size code letter: H, pp. 45-46.

[5] Simoes-Moreira, J. R., 2010, "An air-standard cycle and a thermodynamic perspective on operational limits of Ranque-Hilsch or vortex tubes," Int. J. Refrig., 33, pp. 765-773.

[6] OSHA Regulations (Standards – 29 CFR), Part 1926, 2017, "Safety and Health Regulations for Construction," Occupational Safety and Health Administration, Washington, DC, pp. 35–36.

[7] NIOSH, June 1998, "Criteria for a Recommended Standard: Occupational Noise Exposure, Revised Criteria 1998," National Institute for Occupational Safety and Health, Washington, DC, p. 24.

[8] United States Nuclear Regulatory Commission (U.S.NRC) Regulations (Standards – 10 CFR), Part 20, 2017, "Standards for Protection Against Radiation," p. 344, 365.

[9] SAS Institute, 2014, "JMPTM Pro", Version 11.2.1, SAS Institute, Cary, NC.

[10] Conover, W.J., 1980, *Practical Nonparametric Statistics*, 2nd ed., Wiley, New York.

[11] Taylor Enterprises, 2007, Distribution Analyzer, Version 1.2, Taylor Enterprises, Libertyville, IL.

[12] D'Agostino, R. B., and Stephens, M. A., 1986, *Goodness of Fit Techniques*. Marcel Dekker, Inc., New York, NY

[13] Figliola, R.S., and Beasley, D.E., 2011, *Theory and Design for Mechanical Measurements*, 5th ed., Wiley, New York, pp. 164, 170, 184, 190-192.

[14] Moran, M. J., Shapiro, H. N., Boettner, D. D., and Bailey, M. B., 2011, Fundamentals of Engineering Thermodynamics, 7th ed., Wiley, New York, p. 925.

[15] Vining, G., and Kowalski, S.M., 2011, *Statistical Methods for Engineers*, 3rd ed., Brooks/Cole, Boston, MA, p. 595.